Cluster effects on optical properties of glass–metal nanocomposites

G C DAS[1] and D CHAKRAVORTY[2]

[1]Department of Metallurgical Engineering, Jadavpur University, Calcutta 700 032, India
[2]Indian Association for the Cultivation of Science, Jadavpur, Calcutta 700 032, India

Abstract. Optical absorption characteristics in a glass–metal nanocomposite system involving bismuth metal have been analysed using effective medium theories with a model incorporating single strand chains and *fcc* clusters of metallic bismuth particles. The computed values show fair agreement with experimental data.

1. Introduction

Optical properties of dielectric-metal nanocomposites have attracted considerable attention in recent years (Granqvist and Hunderi 1980) because of their potential application in photothermal energy conversion devices. Nanocomposite films have so far been prepared either by gas evaporation (Granqvist and Buhrman 1976) or by r.f. sputtering (Craighead and Buhrman 1977). The optical absorption characteristics of these materials have been analysed by effective medium theories (Niklasson *et al* 1981) and show reasonable agreement with experimental data. Glass–metal nanocomposites have also been studied earlier (Doremus 1964; Kreibig 1974). Some recent investigations on nanocomposites involving bismuth metal and oxide glasses show interesting memory-switching behaviour (Chakravorty and Murthy 1975). This has been explained as arising due to the formation of a percolation path by the connectivity of stretched metal granules under the influence of an applied electric field (Das and Chakravorty 1980). The extremely low value of the volume fraction of the metal phase (typically in the range 0·03 to 0·12) implies that the interconnectivity is brought about by the bismuth particles which form a minor phase within the glass matrix. This is indicated also from the TEM microstructures (Das and Chakravorty 1982). Optical properties of these nanocomposites have been reported earlier (Das *et al* 1983) and the data analysed by various effective medium theories. In these analyses we have made the assumption that the bismuth metal phase consists of spheres only. On the basis of microstructural characteristics and the switching phenomenon exhibited by the bismuth–metal vanadium–phosphate glass nanocomposites as delineated above, we have reanalysed the optical data by assuming that the metal phase consists of spheres, single strand chains and *fcc* clusters (Granqvist and Hunderi 1977). The agreement between the experimental values of the optical absorption coefficient and those computed as above is found to be much better than that reported earlier (Das *et al* 1983). The results are presented in this paper.

2. Experimental

The starting composition of the glass–metal nanocomposite chosen for the study

is $80V_2O_5-15P_2O_5-5Bi_2O_3$ (mol%). The details of sample preparation, optical absorption measurements and microstructural characterization have been reported earlier (Das *et al* 1983). Figure 1a is the transmission electron micrograph of the specimen used in the present investigation. The sample was subjected to reduction treatment at 200°C for 2 h. The dark regions in this micrograph represent the bismuth-rich phase. The figure describes a two-dimensional projection of bismuth particles distributed in a three-dimensional nanocomposite. The volume fraction of the metal phase has been estimated by considering the thickness of the TEM sample (Das 1982). Figure 1b is the selected area diffraction pattern for the region described by figure 1a. The rings confirm the presence of metallic bismuth in the nanocomposites investigated.

2.1 Calculations

The simplest effective medium theory is the one developed by Maxwell–Garnett (MG) (1904). Polder and Van Santen (PVS) (1946) incorporated Onsager's reaction field to derive an improved effective medium permeability $(\bar{\varepsilon}^{MG-PVS})$ for particles of ellipsoidal shape and is given by

$$\bar{\varepsilon}^{MG-PVS} = \varepsilon_m \frac{1+(2/3)\sum_j f_j \delta_j}{1-(1/3)\sum_j f_j \delta_j} \tag{1}$$

where f_j is the fill factor of particles belonging to the jth class such that $\sum_j f_j = f$, where f is the fill factor, ε_m is the dielectric permeability of the matrix. δ_j is related to polarizability of the particles and is given by (Granqvist and Hunderi 1977)

$$\delta_j = \frac{1}{3} \sum_{k=1}^{3} \left[\frac{\varepsilon_j - \bar{\varepsilon}^{MG-PVS}}{\bar{\varepsilon}^{MG-PVS} + L_k(\varepsilon_j - \bar{\varepsilon}^{MG-PVS})} \right], \tag{2}$$

where L_k are the depolarization factors of particles and ε_j is the size-dependent dielectric permittivity. The frequency (ω) dependent optical absorption coefficient is given by (Granqvist and Hunderi 1977)

$$\alpha(\omega)^{MG-PVS} = (\omega/c) [\bar{\varepsilon}_2/\bar{\varepsilon}_1^{\frac{1}{2}}], \tag{3}$$

where $\bar{\varepsilon}_2$ and $\bar{\varepsilon}_1$ are the imaginary and real parts of dielectric permittivity of (1).

For reasons given earlier, we assume that the bismuth phase contains ξ fraction of spheres, ζ fraction of single strand chains and $\chi(=1-\xi-\zeta)$ fraction of fcc clusters. The effect of these geometrical configurations can be incorporated in the MG–PVS theory by suitably replacing L_k in (2). Our objective is to find the optimum combination of ξ, ζ and χ to get the best agreement with experimental results. It is evident that any two of these can be taken as the adjustable parameters in fitting the absorption spectra. So the objective function to be minimised is given by

$$f(\mathbf{X}) = \sum_{\omega=1}^{n} \left[\alpha(\omega)^{MG-PVS} - \alpha(\omega)^{Expt.} \right]^2. \tag{4}$$
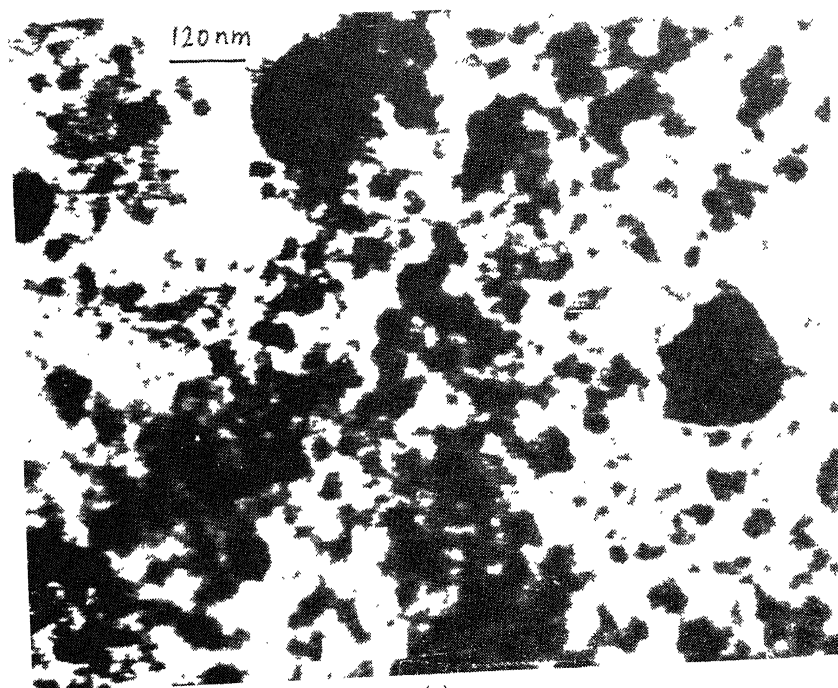
(a)
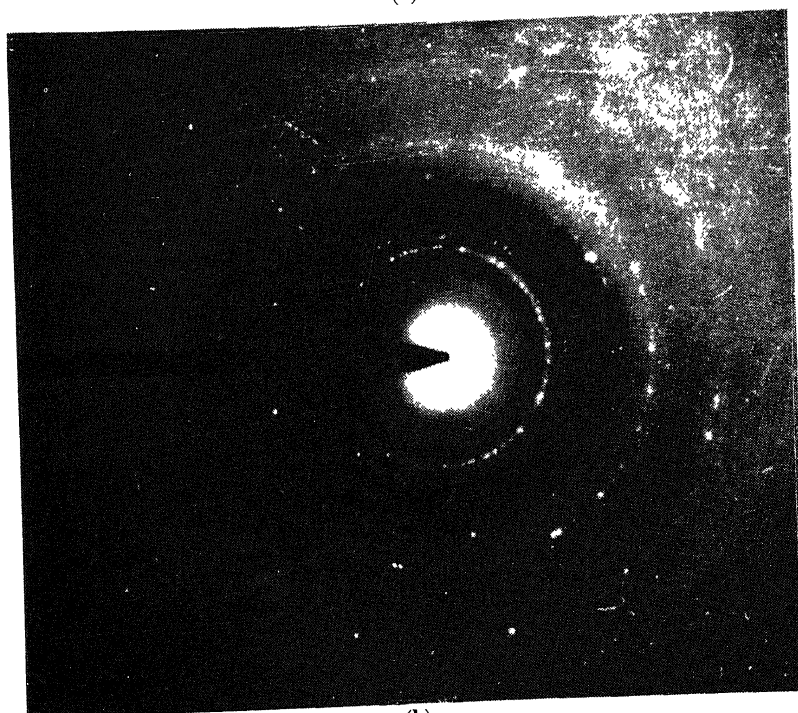
(b)

Figure 1. (a) Transmission electron micrograph for a glass of composition $80V_2O_5$–$15P_2O_5$–$5Bi_2O_3$ (mol%) reduced at 200°C for 2 h. (b) Selected area diffraction pattern for the micrograph in figure 1a.

Subject to constraints,

$$\left.\begin{array}{c} \xi \geqslant 0 \\ \zeta \geqslant 0 \\ \xi + \zeta \leqslant 1 \end{array}\right\}, \tag{5}$$

where, $\mathbf{X}$ is the vector consisting of ξ and ζ, the optimization variables. The above constrained optimization is converted into an equivalent unconstrained optimization by augmenting the function $f(\mathbf{X})$ by a penalty term within the frame work of interior penalty function method (Rao 1979). The equivalent function $\phi(\mathbf{X}, r_k)$ is given by,

$$\phi(\mathbf{X}, r_k) = f(\mathbf{X}) - r_k \sum_{j=1}^{m} \frac{1}{g_j(\mathbf{X})}, \tag{6}$$

where, r_k is the penalty parameter and $g_j(\mathbf{X}) \leqslant 0$ is the constraint. In our case,

$$\sum_{j=1}^{m} \frac{1}{g_j(\mathbf{X})} = \left[-\frac{1}{\xi} - \frac{1}{\zeta} + \frac{1}{\xi + \zeta - 1} \right]. \tag{7}$$

In order to calculate $f(\bar{X})$ from (4), we have to find an expression for $\bar{\varepsilon}_1$ and $\bar{\varepsilon}_2$. Separating the real and imaginary parts in (1) we get,

$$\bar{\varepsilon}_1 = \varepsilon_m \frac{A_1 C_1 - B_1 D_1}{C_1^2 + D_1^2}, \tag{8}$$

$$\bar{\varepsilon}_2 = \varepsilon_m \frac{B_1 C_1 + A_1 D_1}{C_1^2 + D_1^2}, \tag{9}$$

where, A_1, B_1, C_1 and D_1 are given by,

$$A_1 = 1 + \frac{2}{3} f \left[\xi \sum_j \omega_j \delta'_{j\,|\text{sphere}} + \zeta \delta'_{|\text{s.c.}} + \chi \delta'_{|\text{f.c.}} \right] \tag{10}$$

$$B_1 = \frac{2}{3} f \left[\xi \sum_j \omega_j \delta''_{j\,|\text{sphere}} + \zeta \delta''_{|\text{s.c.}} + \chi \delta''_{|\text{f.c.}} \right] \tag{11}$$

$$C_1 = 1 - \frac{1}{3} f \left[\xi \sum_j \omega_j \delta'_{j\,|\text{sphere}} + \zeta \delta'_{|\text{s.c.}} + \chi \delta'_{|\text{f.c.}} \right] \tag{12}$$

$$D_1 = \frac{1}{3} f \left[\xi \sum_j \omega_j \delta''_{j\,|\text{sphere}} + \zeta \delta''_{|\text{s.c.}} + \chi \delta''_{|\text{f.c.}} \right] \tag{13}$$

For (10) to (13) the subscripts, sphere, s.c. and f.c. stand for sphere, single strand chain and *fcc* clusters of the bismuth phase, respectively.

ω_j is the weight factor and is given by,

$$\omega_j = \frac{x_j^3 n_j}{\Sigma x_j^3 n_j} \quad \text{and} f_j = f\omega_j. \tag{14}$$

x_j and n_j are particle size and number of particles in jth class. δ'_j and δ''_j of the above equations are obtained by separating real and imaginary parts of (2) and are given by,

$$\delta'_j = \frac{1}{3} \sum_{k=1}^{3} \frac{EG_k + FH_k}{G_k^2 + H_k^2}, \tag{15}$$

$$\delta''_j = \frac{1}{3} \sum_{k=1}^{3} \frac{FG_k - EH_k}{G_k^2 + H_k^2}, \tag{16}$$

where,

$$E = \varepsilon'_j - \bar{\varepsilon}_1, \tag{17}$$

$$F = \varepsilon''_j - \bar{\varepsilon}_2, \tag{18}$$

$$G_k = L_k \varepsilon'_j + (1 - L_k)\bar{\varepsilon}_1, \tag{19}$$

$$H_k = L_k \varepsilon''_j + (1 - L_k)\bar{\varepsilon}_2, \tag{20}$$

where ε'_j and ε''_j are the size and frequency-dependent real and imaginary parts respectively of dielectric constants of the metallic phase (Das *et al* 1983). For evaluating δ'_j and δ''_j for sphere, we have taken the depolarization factors as $L_1 = L_2 = L_3 = 1/3$ (Granqvist and Hunderi 1977). We also assume that the different geometrical configurations are made of identical spheres. Therefore to calculate δ' and δ'' for s.c. and f.c. we have used an average particle size computed from the TEM photograph. The effective depolarizations factors (L_1, L_2 and L_3) used for s.c. and f.c. configurations are respectively 0·133, 0·435 and 0·435; 0·0865, 0·0865 and 0·827 (Granqvist and Hunderi 1977).

To compute $\bar{\varepsilon}_1$ and $\bar{\varepsilon}_2$ from (8) and (9) we have to compute δ'_j and δ''_j which are functions of $\bar{\varepsilon}_1$ and $\bar{\varepsilon}_2$. Therefore $\bar{\varepsilon}_1$ and $\bar{\varepsilon}_2$ have to be computed by the following iterative method. First we assume the values of $\bar{\varepsilon}_1$ and $\bar{\varepsilon}_2$ to be given by

$$\bar{\varepsilon}_1^{(0)} = \varepsilon_m \text{ and } \varepsilon_2^{(0)} = 0.$$

With these values we calculate

$$\bar{\varepsilon}_1^{(1)} = F_1 (\bar{\varepsilon}_1^{(0)}, \bar{\varepsilon}_2^{(0)}), \tag{21}$$

$$\bar{\varepsilon}_2^{(1)} = F_2 (\bar{\varepsilon}_1^{(0)}, \varepsilon_2^{(0)}). \tag{22}$$

The exact functional forms of (21) and (22) are defined by (8) to (20). Here the superscript indicates the number of iterations. Substituting $\bar{\varepsilon}_1^{(1)}$ and $\bar{\varepsilon}_2^{(1)}$ in (21) and (22) we get $\bar{\varepsilon}_1^{(2)}$ and $\bar{\varepsilon}_2^{(2)}$ and so on. So in the ith iteration,

$$\bar{\varepsilon}_1^{(i)} = F_1 (\bar{\varepsilon}_1^{(i-1)}, \bar{\varepsilon}_2^{(i-1)}), \tag{21a}$$

$$\bar{\varepsilon}_2^{(i)} = F_2 (\bar{\varepsilon}_1^{(i-1)}, \bar{\varepsilon}_2^{(i-1)}), \tag{22a}$$

This iteration is continued until the difference between the two successive iterations is less than a pre-assigned positive quantity e, i.e. when simultaneously,

$$|\bar{\varepsilon}_1^{(i)} - \bar{\varepsilon}_1^{(i-1)}| < e,$$

$$\text{and} \quad |\bar{\varepsilon}_2^{(i)} - \bar{\varepsilon}_2^{(i-1)}| < e.$$

Here in our problem we have chosen $e = 0.1$.

The computed values of $\bar{\varepsilon}_1$ and $\bar{\varepsilon}_2$ are substituted in (3) to calculate the frequency dependent $\alpha(\omega)$. This in turn is substituted in (4) to compute the value of $f(x)$.

The following iterative scheme has been used to optimize the function $f(X)$ subject to the constraints as mentioned earlier within an error of $\pm 4\%$.

Step 1: The computation is started with three initial feasible points X_1, X_2 and X_3 (to define the initial simplex) such that strictly the constraints $g_j(X_i) < 0$ for $i = 1$ to 3 and $j = 1$ to 3 are satisfied;
set $K \leftarrow 1$ and take $r_k > 0$.

Step 2: $\phi(X, r_k)$ is minimised using simplex optimization technique (Rao 1979) and the centroid of the latest simplex X_k^* for which convergence criterion is satisfied is taken as the optimum point.

Step 3: If $K \neq 1$, go to step 5.

Step 4: Set $F_1 \leftarrow F(X_k^*)$ and go to step 8.

Step 5: Set $F_2 \leftarrow F(X^*)$

Step 6: If $\left| \dfrac{F_2 - F_1}{F_2} \right| \leqslant \varepsilon$ go to step 10.

In our problem $\varepsilon = 0.04$ is assigned.

Step 7: Set $F_1 \leftarrow F_2$

Step 8: Compute the new penalty parameter
$r_{k+1} = cr_k$, where $c < 1$

Step 9: Take X_{k1}^*, X_{k2}^* and X_{k3}^* points of the latest simplex, as the starting points. Set $K \leftarrow K + 1$ and repeat step 2.

Step 10: Take X_k^* as the optimum vector.

Step 11: Compute $\alpha(\omega)^{MG-PVS}$ by using (3) at X_k^*.

Step 12: Stop.

Based on the above algorithm a programme in FORTRAN language has been written (Das 1982) and run on the DEC system 1090.

3. Discussion

Figure 2 shows the plot of α values as the function of wavelength λ for $80V_2O_5$–$15P_2O_5$–$5Bi_2O_3$ (mol%) glass films reduced at $200°C$ for 2 h. The optimum combination of geometrical configurations of the metallic bismuth phase is found to be 26% sphere, 1% single strand chains and 73% fcc clusters. The fill factor and the average particle size $\bar{X}$ of the metallic phase in this composite as computed from electron micrographs are 0·033 and 10 nm respectively. The entire region of spectrum is not in a non-dispersive region, but the effective medium theories invoked here are not dependent on this property of the metal phase. In figure 2 are
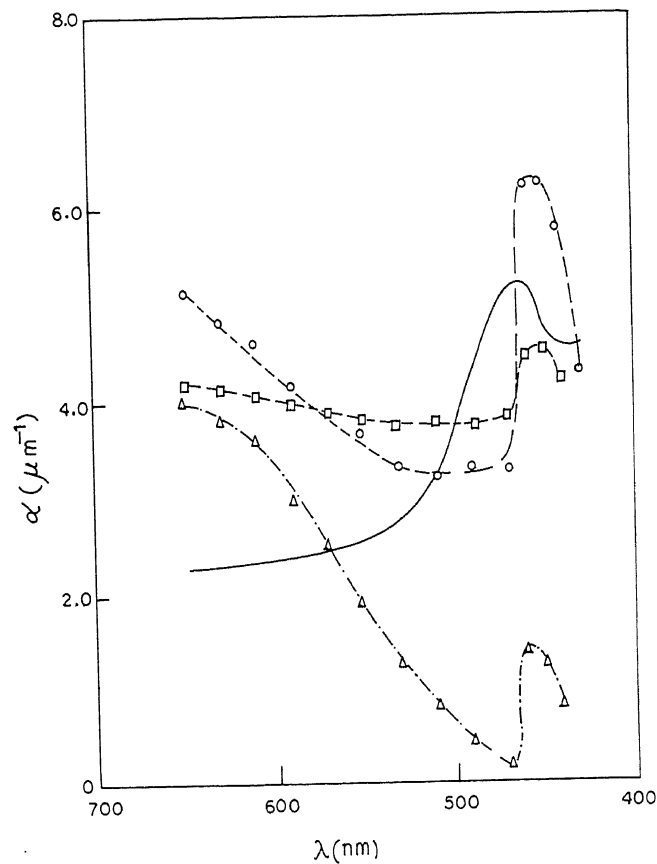
Figure 2. Comparison of experimental absorption coefficient α as a function of wavelength with theoretical values computed by different models for glass-metal nanocomposite thin films reduced at 200°C for 2 h. Glass composition: $80V_2O_5-15P_2O_5-5Bi_2O_3$ (mol%), $f=0.033$, $\bar{X}=10$ nm. ($-$ Experimental; $\bigcirc$ MG theory; $\triangle$ MG-PVS theory; $\square$ constrained optimization.)

also shown the curves as computed by MG and MG-PVS theories, assuming the particles to consist of spheres only, and also the experimental curve for the purpose of comparison. It is evident that the curve as obtained by the optimization technique is a much better fit to the experimental data than that predicted by either the MG or the MG-PVS theory. The presence of *fcc* clusters and single strand chains formed by the metallic bismuth phase in the nanocomposite under investigation therefore makes the particle stretching model for memory switching (Das and Chakravorty 1980) a realistic proposition.

Acknowledgement

References

Chakravorty D and Murthy C S 1975 *J. Phys.* **D8** L162
Craighead H G and Buhrman R A 1977 *Appl. Phys. Lett.* **31** 423
Das G C 1982 *Memory switching and optical properties of glass–metal microcomposites*, Ph.D. thesis, Indian Institute of Technology, Kanpur
Das G C and Chakravorty D 1980 *J. Appl. Phys.* **51** 3896
Das G C and Chakravorty D 1982 *J. Phys.* **D15** 2255
Das G C, Das R and Chakravorty D 1983 *Bull. Mater. Sci.* **5** 277
Doremus R H 1964 *J. Chem. Phys.* **40** 2389
Granqvist C G and Buhrman R A 1976 *J. Appl. Phys.* **47** 2200
Granqvist C G and Hunderi O 1977 *Phys. Rev.* **B16** 3513
Granqvist C G and Hunderi O 1980 *J. Appl. Phys.* **51** 1751
Kreibig U 1974 *J. Phys.* **F4** 999
Maxwell-Garnett J C 1904 *Philos. Trans. R. Soc. (London)* **203** 385
Niklasson G A, Granqvist C G and Hunderi O 1981 *Appl. Opt.* **20** 26
Polder D and Van Santen 1946 *Physica (Utrecht)* **12** 257
Rao S S 1979 *Optimization theory and practice* (New Delhi: Wiley Eastern)